

Regulation of bone and fat balance by fructus ligustri lucidi in ovariectomized mice

Xiao-Yan Qin^{1,2}, Qiu Wei^{1,2}, Yun Yang^{1,2}, Ran An^{1,2}, Xiao-Ling Han^{1,2}, Hao-Ping Mao^{1,2}

¹Tianjin University of Traditional Chinese Medicine, Tianjin, China

²Tianjin State Key Laboratory of Modern Chinese Medicine, Tianjin University of Traditional Chinese Medicine, Tianjin, China

Correspondence to: Hao-Ping Mao; email: maohaoping@tjutcm.edu.cn

Keywords: *Fructus Ligustri Lucidi* (FLL), ovariectomy, osteoclast, adipogenesis, postmenopausal osteoporosis

Received: March 11, 2021

Accepted: August 24, 2021

Published:

Copyright: © 2021 Qin et al. This is an open access article distributed under the terms of the [Creative Commons Attribution License](https://creativecommons.org/licenses/by/3.0/) (CC BY 3.0), which permits unrestricted use, distribution, and reproduction in any medium, provided the original author and source are credited.

ABSTRACT

Fructus Ligustri Lucidi, a traditional Chinese medicine, is the fruit of *Ligustrum lucidum* Ait. (Oleaceae). It has invigorating effects on the liver and kidneys and is a commonly used herb in the treatment of age-related diseases. The ethanol extract of FLL is a potential candidate for the prevention and treatment of postmenopausal osteoporosis. In the present study, we aimed to determine whether the ethanol extract of FLL yields an anti-osteoporotic effect on ovariectomized mice and to explore the relevant underlying mechanisms of action. One week after surgery, animals were randomly assigned to five groups, at 10 per group: a sham group, OVX group, E2 group, and FLL group (2 g/kg and 4 g/kg). Eight weeks after treatment, we harvested the uteri, femurs, tibias, visceral organs, and plasma from the mice. The levels of estradiol, Trap, Trap5b, OPG, and RANKL in plasma were determined by ELISA. We assessed bone mineral density and bone microstructure by X-ray absorptiometry and micro-CT, and the formation of F-actin rings was detected by immunofluorescence staining assay. FLL significantly decreased osteoclast activity, increased bone mineral density, and improved bone microstructure in OVX mice ($P < 0.05$). The fat content of abdominal fat and bone marrow were also reduced after treatment with FLL ($P < 0.01$). In addition, FLL (1 $\mu\text{g}/\text{mL}$) suppressed the formation of osteoclasts and F-actin rings *in vitro* ($P < 0.01$). FLL inhibited adipocyte differentiation in both fate determination and maturation from monocytes by inhibiting Zfp423 and PPAR γ mRNAs ($P < 0.01$ or $P < 0.05$). In summary, FLL prevented additional bone loss and improved bone microstructure in OVX mice by suppressing the activity of osteoclasts and reducing the fat content in the abdomen and the bone marrow.

INTRODUCTION

Menopause is a natural part of aging in women who are in a transitional phase from reproductive to non-reproductive status. This area holds significant research interest, as some common menopause-related metabolic diseases occur in postmenopausal women, such as osteoporosis and obesity. Osteoporosis exerts a substantial impact on the quality of life in postmenopausal women since osteoporosis-related fractures constitute the primary cause of disability or even death among the elderly female population. It has

been estimated that nearly half of all postmenopausal women will undergo one osteoporotic fracture in their lifetime [1]. There are also reports of obesity and increased numbers of bone marrow adipocytes in menopausal women. Despite our previous conventional reasoning that obesity protected against osteoporotic fractures because of peripheral adiposity providing insulation in falls, the belief that obesity is protective against osteoporosis has recently been revised [2]. Too much intra-abdominal fat, visceral obesity, or bone marrow yellow fat are reported to be harmful for bone health [3], and postmenopausal women are at an

increased risk of developing visceral obesity and intra-abdominal fat [4]. Hence, the interregulation between bone and fatty tissue may provide a potential means to investigate various medications for use in postmenopausal osteoporosis. *Fructus Ligustri Lucidi* (FLL) was originally described by Shen Nong Ben Cao Jing as a means to nourish the yin and supplement the kidneys. Previous studies revealed that extracts of FLL possess significant therapeutic properties such as providing anti-tumor activities, hepatoprotection, immunoregulation, anti-inflammation, and amelioration of hyperlipidemia [5]. The previous experimental results of our research group found that Erzhi formula (consists of *Ecliptae herba* and *Fructus Ligustri Lucidi* at a ratio 1:1) significantly inhibited the bone loss induced by OVX in mice by its regulation of estradiol combined with the nourishing effect of the uterus, and that it also attenuated bone resorption by decreasing the RANKL/OPG ratio so as to inhibit osteoclast maturation [6]. It demonstrated that FLL has a certain effect of anti-osteoporosis, but a beneficial effect on bone has not yet been shown scientifically.

Thus, the current study was carried out on ovariectomized mice, a model of surgical post-menopause, in order to elucidate the impact of FLL on bone and fat tissues in postmenopausal osteoporosis. These results are expected to present important therapeutic and preventive implications for women in the menopause and post-menopausal period.

RESULTS

FLL suppresses uterine atrophy induced by OVX

We successfully established the OVX-mouse model, and validated it by measuring the levels of estradiol in plasma. Our results showed that the estradiol levels were significantly decreased one week after OVX in all mice, indicating the success of the surgical procedure ($P < 0.01$; Figure 1A). Our results also showed that uterine atrophy was prominent in OVX mice and that the uterine weights in the model group were significantly reduced ($P < 0.01$). Estrogen and FLL treatment reversed uterine atrophy and significantly augmented uterine weight ($P < 0.05$; Figure 1B).

FLL suppresses the loss of bone and reduces fat weight in OVX mice

Our data revealed that OVX significantly increased body weights in OVX mice at the end of the study, while treatment with FLL significantly reduced the weight gained ($P < 0.05$; Figure 2A); and the changes in body weight were independent of daily diet ($P > 0.05$; Table 1). We also measured the weights of various organs—including bone, fat issue, lean body mass, liver, spleen, and kidney in the mice after treatment with FLL for 8 weeks. Results from dual-energy X-ray absorptiometry showed that the BMD in the femurs of

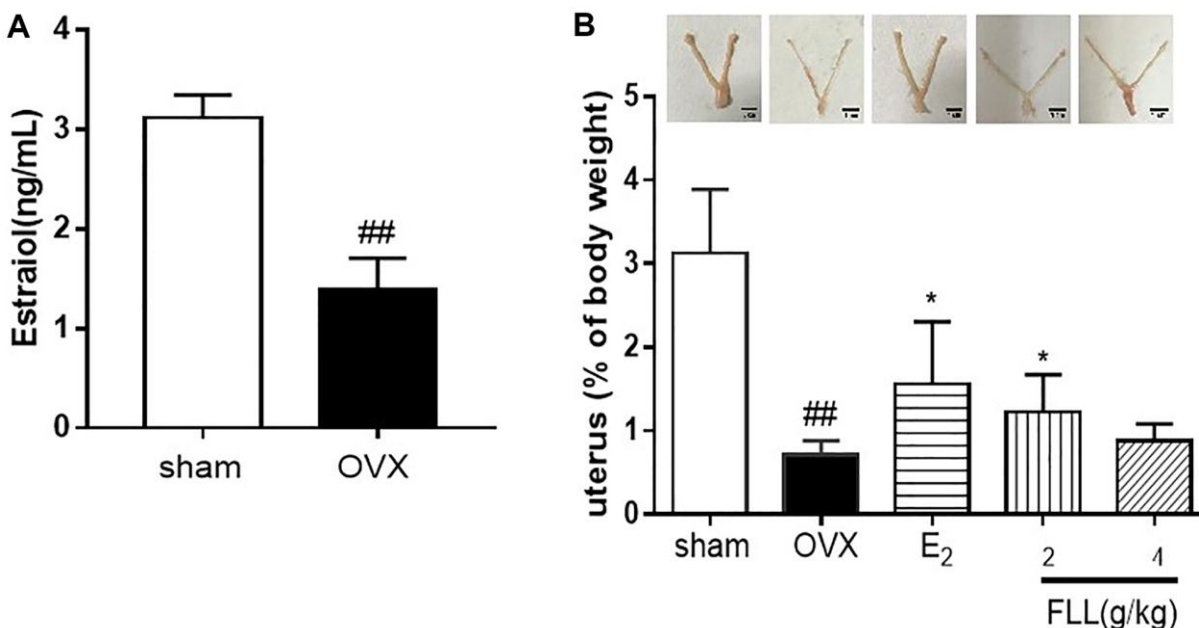


Figure 1. FLL suppresses uterine atrophy induced by OVX. (A) Estradiol concentrations were significantly diminished one week after OVX in all mice as detected by ELISA kit. (B) Uterine atrophy in OVX mice after treatment with FLL at 8 weeks. ## $P < 0.01$ compared with sham; * $P < 0.05$ compared OVX ($n = 10$).

Table 1. The daily diet of mice.

Groups	Days	Daily diet (g)
sham	60	2.80 ± 0.43
OVX	60	2.78 ± 0.36
E2	60	2.78 ± 0.49
FLL (2 g/kg)	60	2.97 ± 0.53
FLL (4 g/kg)	60	2.75 ± 0.38

OVX mice was significantly diminished compared to the sham group ($P < 0.01$; Figure 2B), and that E2 and FLL (2 g/kg) significantly elevated BMD in OVX mice ($P < 0.01$ or 0.05 ; Figure 2B). When we determined body fat and lean content of each group by the NMR body-composition analyzer, we observed that 8 weeks after OVX surgery the fat content

obviously increased in OVX mice, while it significantly decreased in the E2 and FLL groups compared with the same indices in the OVX group ($P < 0.01$ or 0.05 ; Figure 2C). There was no difference in lean content among groups (Figure 2D); and we uncovered no differences in the indices for the liver, kidney and spleen among groups (Figure 2E–2G).

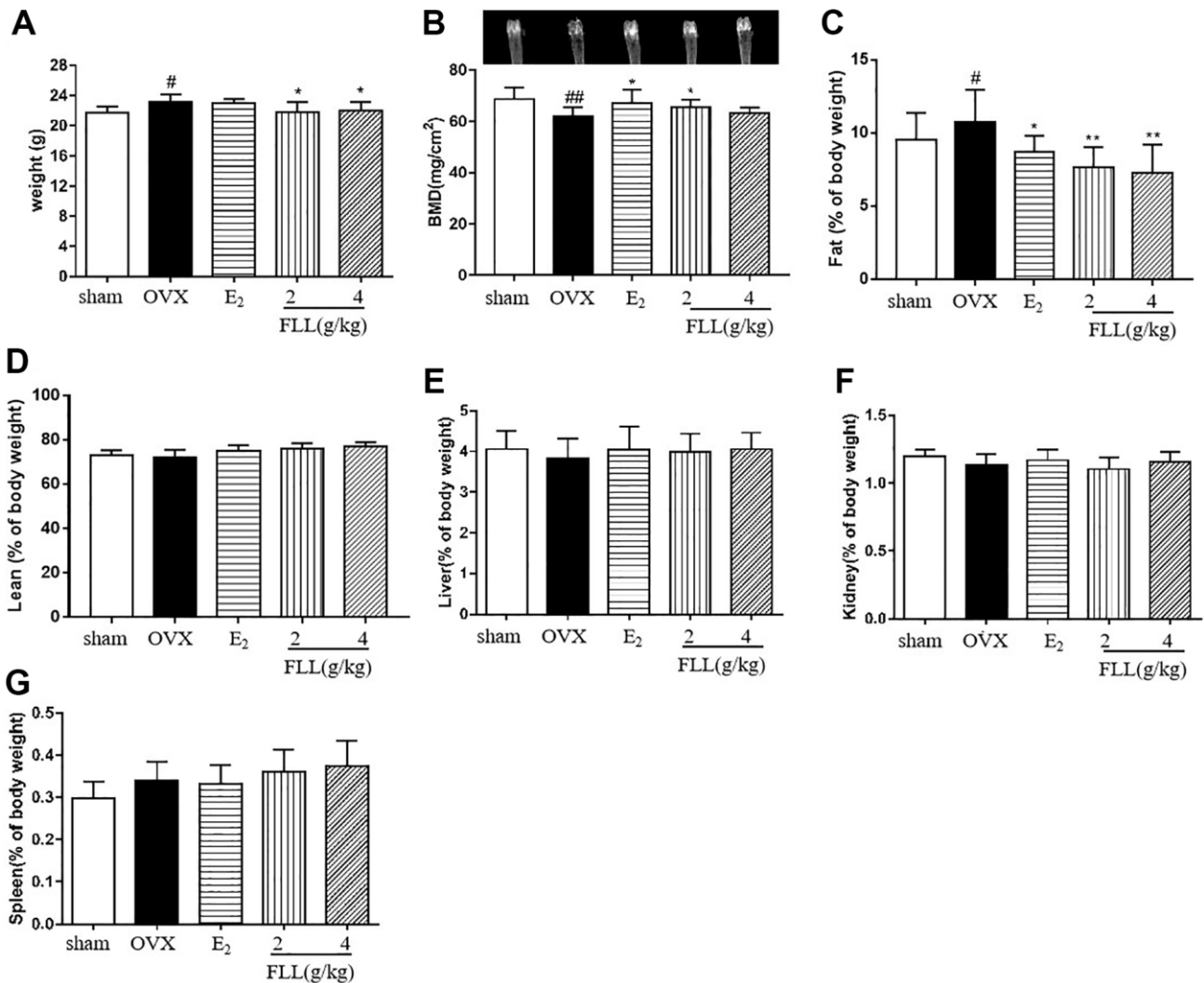


Figure 2. FLL suppresses bone loss and reduces fat weight in OVX mice. (A) Body weights of OVX mice 8 weeks post-operatively. Treatment with FLL decreased body weight significantly. (B) Bone mineral density (BMD) in the femurs of OVX mice decreased significantly compared to the sham group, and estrogen and FLL significantly augmented BMD in OVX mice. The body fat and (C) lean content (D) of each group were evaluated by NMR body composition analyzer after 8 weeks. (E–G) The indices for liver, kidney and spleen among groups. # $P < 0.05$ compared with sham; ## $P < 0.01$ compared with sham; * $P < 0.05$ compared OVX; ** $P < 0.01$ compared OVX ($n = 10$).

FLL improves bone microstructure and mechanical properties, and reduces fat content in the bone marrow of OVX mice

Since FLL significantly suppressed the loss of bone in OVX mice, we evaluated the microstructure of the distal femur by micro-CT. Microstructural parameters of the trabecular bone in the distal femur showed that Conn.D in the OVX group was significantly lower than in the sham group ($P < 0.01$); however, E2 and FLL (2 g/kg) reversed the changes induced by OVX in Conn.D ($P < 0.01$ or 0.05; Figure 3A and 3B). In addition, left tibial strength was significantly diminished in the OVX group ($P < 0.01$) but dramatically increased in the FLL group (2 g/kg) ($P < 0.05$; Figure 3C). OPG plays a crucial role in preventing osteoporosis and RANKL binds to OPG, inhibiting the formation of osteoclasts by disrupting RANKL-RANK signaling. The level of OPG significantly increased in the FLL group compared to the OVX group ($P < 0.05$), and commensurately inhibited the level of RANKL ($P < 0.01$) (Figure 4A and 4B). The ratio of OPG/RANKL was significantly reduced in the OVX group, while it was significantly elevated after treatment with FLL ($P < 0.01$; Figure 4C). Results for OPG and RANKL proteins in bone tissue were consistent with the results from plasma (Figure 4D and 4E). Using H&E staining of femurs, we also found that the adipose tissue that we observed as white vacuoles in bone marrow increased in the OVX group,

while E2 and FLL significantly reduced the area of white vacuolation after 8 weeks of treatment in OVX mice ($P < 0.01$; Figure 5A and 5B).

FLL inhibits osteoclastogenesis and function by downregulating Trap activity and levels of Trap5b and NFATc1

The levels of Trap activity and Trap5b proteins in plasma represent clinical osteoclast activity. Our study showed that Trap activity and the level of Trap5b protein were significantly increased in the OVX group, and that treatment with FLL significantly inhibited these increases ($P < 0.01$; Figure 6A and 6B). ACP5 and NFATc1 are two key markers of osteoclastogenesis, and our results showed that their mRNA expression in the OVX group was significantly higher than the expression in the sham group. E2 and FLL then suppressed the increase in ACP5 and NFATc1 mRNA expression, respectively ($P < 0.05$ or 0.01; Figure 6C and 6D). When we isolated monocytes from bone marrow to clarify the effect of FLL on osteoclast differentiation and function, we observed that FLL significantly suppressed Trap activity without changing overall cellular activity as determined by CCK-8 assay (Figure 6E and 6F). We also noted that RANKL and M-CSF stimulated the formation of osteoclasts using Trap staining, while FLL inhibited osteoclast differentiation (Figure 6G). F-actin staining

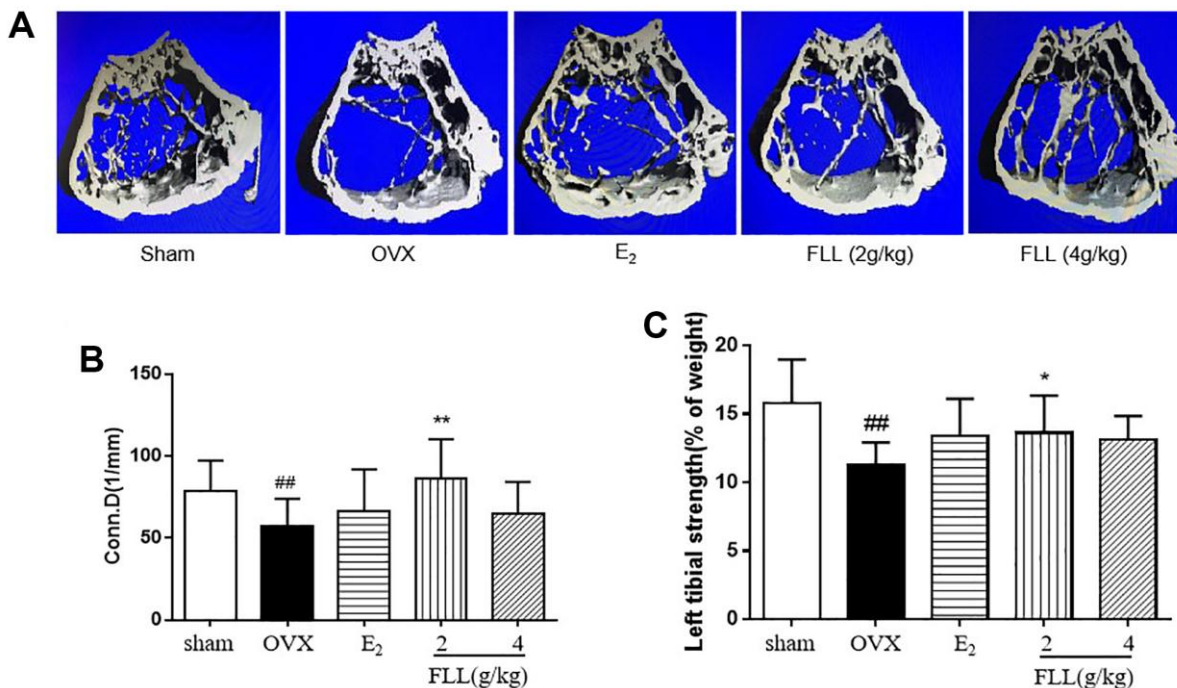


Figure 3. FLL improves bone microstructure and mechanical properties in OVX mice. (A) The microstructure of the distal femur by micro-CT showed that trabecular bone was severely reduced in the model group but recovered with estrogen and FLL treatment. Conn.D (bone trabecular connection density) (B) and left tibial strength (C) in the model group were significantly lower than in the sham group but recovered with 2g/kg of FLL. ### $P < 0.01$ compared with sham; * $P < 0.05$ compared with OVX; ** $P < 0.01$ compared with OVX ($n = 10$).

showed that FLL decreased the formation of F-actin rings (Figure 6H).

Regulation by FLL of MSC differentiation to osteoblasts and adipocytes

Bone marrow mesenchymal stem cells (MSCs) were used to induce osteoblast differentiation and adipocyte differentiation. Our results revealed that FLL

significantly stimulated osteoblast differentiation and the production of ALP while inhibiting adipocyte differentiation and without changing cellular activity as reflected by CCK8 ($P < 0.05$; Figure 7A–7E). We then used the TOPFlash assay to investigate the activation of the Wnt-signaling pathway by FLL, and showed that FLL significantly activated Wnt signaling ($P < 0.01$; Figure 7F). As the principal markers of MSC differentiation into osteoblasts and adipocytes, we

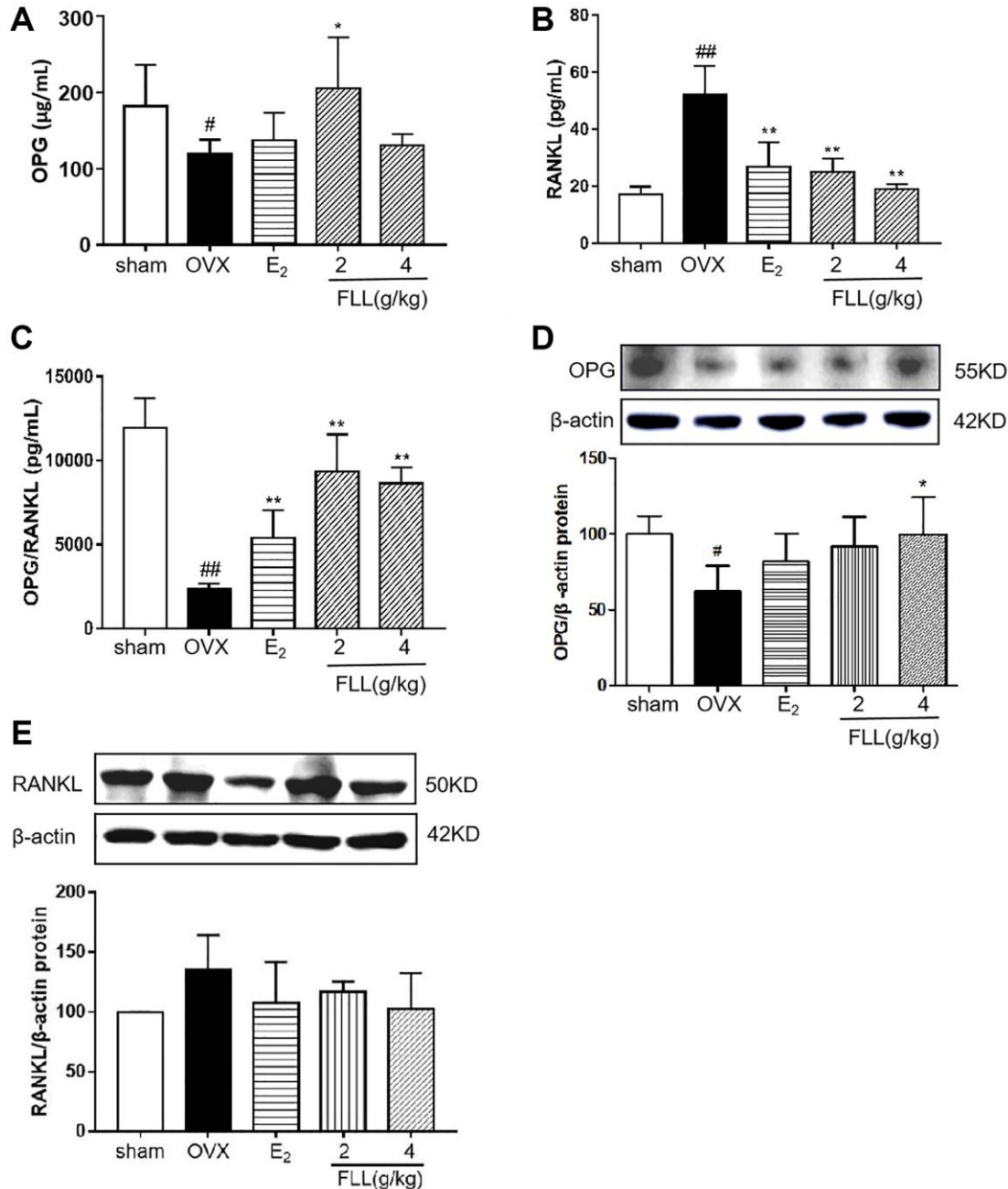


Figure 4. FLL promotes the expression of OPG and inhibits the expression of RANKL in OVX mice. Plasma levels of OPG (A) and RANKL (B) were measured by ELISA. The level of OPG significantly increased in the FLL group compared to the OVX group, and the level of RANKL was commensurately attenuated. (C) The ratio of OPG/RANKL was significantly reduced in the OVX group, while it significantly increased after treatment with FLL ($n = 10$). (D–E) FLL treatment promoted OPG and inhibited RANKL proteins in bone tissue. $^{\#}P < 0.05$ compared with sham; $^{\#\#}P < 0.01$ compared with sham; $^*P < 0.05$ compared with OVX; $^{**}P < 0.01$ compared OVX ($n = 3$).

determined the protein levels of RUNX2 and PPAR γ in bone tissues by western immunoblotting analysis. We observed consistency in the effects of FLL on MSC differentiation, as FLL inhibited PPAR γ expression but stimulated RUNX2 expression ($P < 0.01$ or 0.05 ; Figure 7G–7J).

FLL inhibits fate determination and maturation of adipocytes

Zinc-finger protein 423 (Zfp423) is an important marker of pre-adipocytes, and we found that incubation with an adipocyte-inducer solution for 1 day significantly increased Zfp423 mRNA expression ($P < 0.01$; Figure 8A). PPAR γ is a marker of mature adipocytes, and when we evaluated the effect of FLL on PPAR γ mRNA expression, we observed that incubation with FLL for 7 days significantly inhibited the increase in PPAR γ mRNA that was prompted by the adipocyte-inducer solution ($P < 0.05$; Figure 8B–8D).

DISCUSSION

Postmenopausal osteoporosis (PMOP) is defined as a metabolic bone disease characterized by decreasing bone mineral density and increasing risk of fracture in

postmenopausal women, and is produced by a reduction in circulating estrogen. OVX animals are used worldwide to investigate the physiologic and pathologic changes in postmenopausal women, and the OVX model is used in classic pharmacologic research on PMOP [7]. The current treatment principle with respect to osteoporosis in Western medicine primarily relies on inhibiting bone resorption, promoting bone formation, and increasing bone mineral density. Treatment drugs principally include estrogenic substances, bisphosphonates, parathyroid hormone, vegetarians, calcium, and vitamin D [8–10]. However, Western medical treatment produces a high incidence of adverse reactions and complications—such as stroke, cancer, and cardiovascular disease—and it also shows characteristics of poor prognosis. In addition, Western medicine is typically expensive, which increases the medical burden on patients [11–13]. Therefore, it is of critical importance to adopt novel treatment methods to reduce the harm caused by osteoporosis. There is no concept of osteoporosis in traditional Chinese medicine (TCM), but it is rather spoken of as “bone atrophy” and “bone dryness.” The TCM theory asserts that “the kidneys govern the bone marrow of the body”; i.e., the kidneys store the essence and produce the marrow, and the marrow resides in the bone cavity in order to

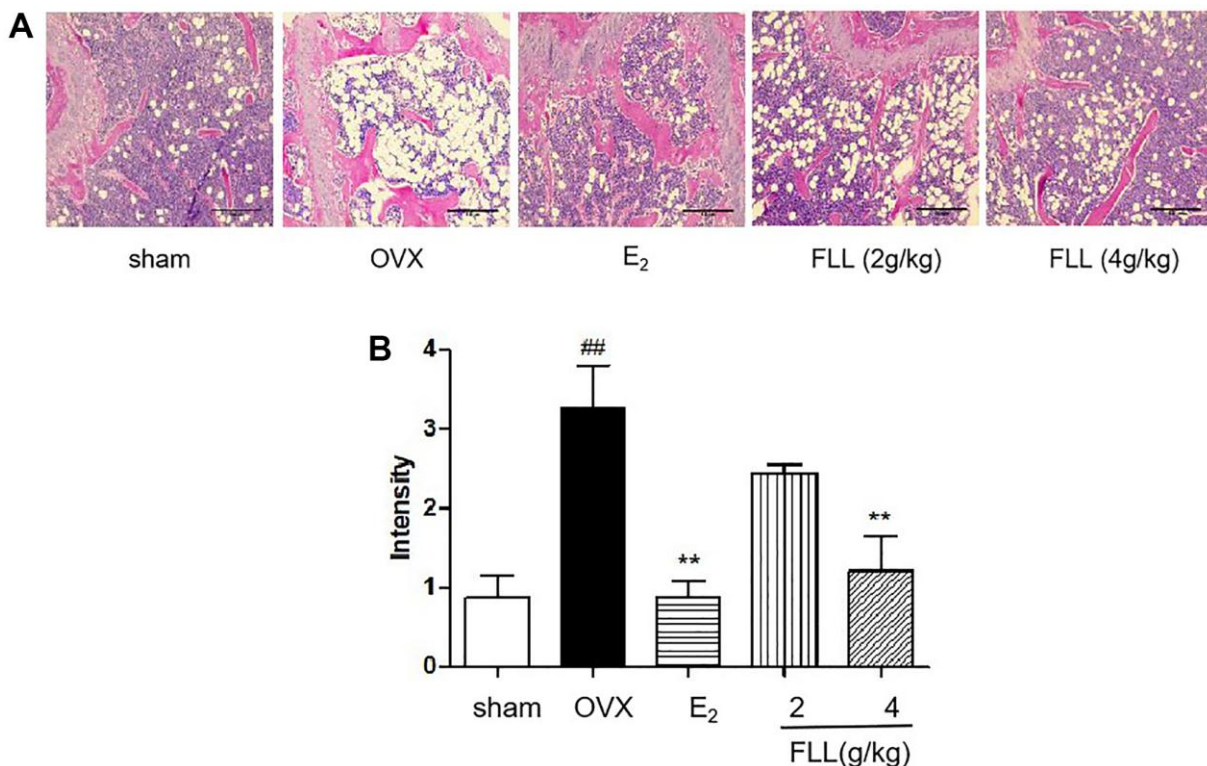


Figure 5. FLL reduces fat content in the bone marrow of OVX mice. (A) H&E staining showed that the white vacuoles in bone marrow increased in the OVX group, while estrogen and FLL significantly reduced the area of white vacuoles after eight weeks of treatment in OVX mice. (B) The white vacuoles were measured quantitatively and data are shown below. ## $P < 0.01$ compared with sham; ** $P < 0.01$ compared with OVX ($n = 3$).

nourish the bones. When the kidney essence is deficient, the bones and marrow are reduced; thus, the kidneys play significant roles in the growth and development of bones. TCM treatment of OP has gradually developed into an important method that engenders significant positive actions with low side effects. More recent

studies have shown that most kidney-tonifying Chinese medicines have estrogen-like effects, which can then regulate bone metabolism and thus exert an anti-osteoporotic action in the postmenopausal period [14]. *Fructus Ligustri Lucidi* as a kidney-tonifying Chinese medicine nourishes the liver and kidneys, and improves

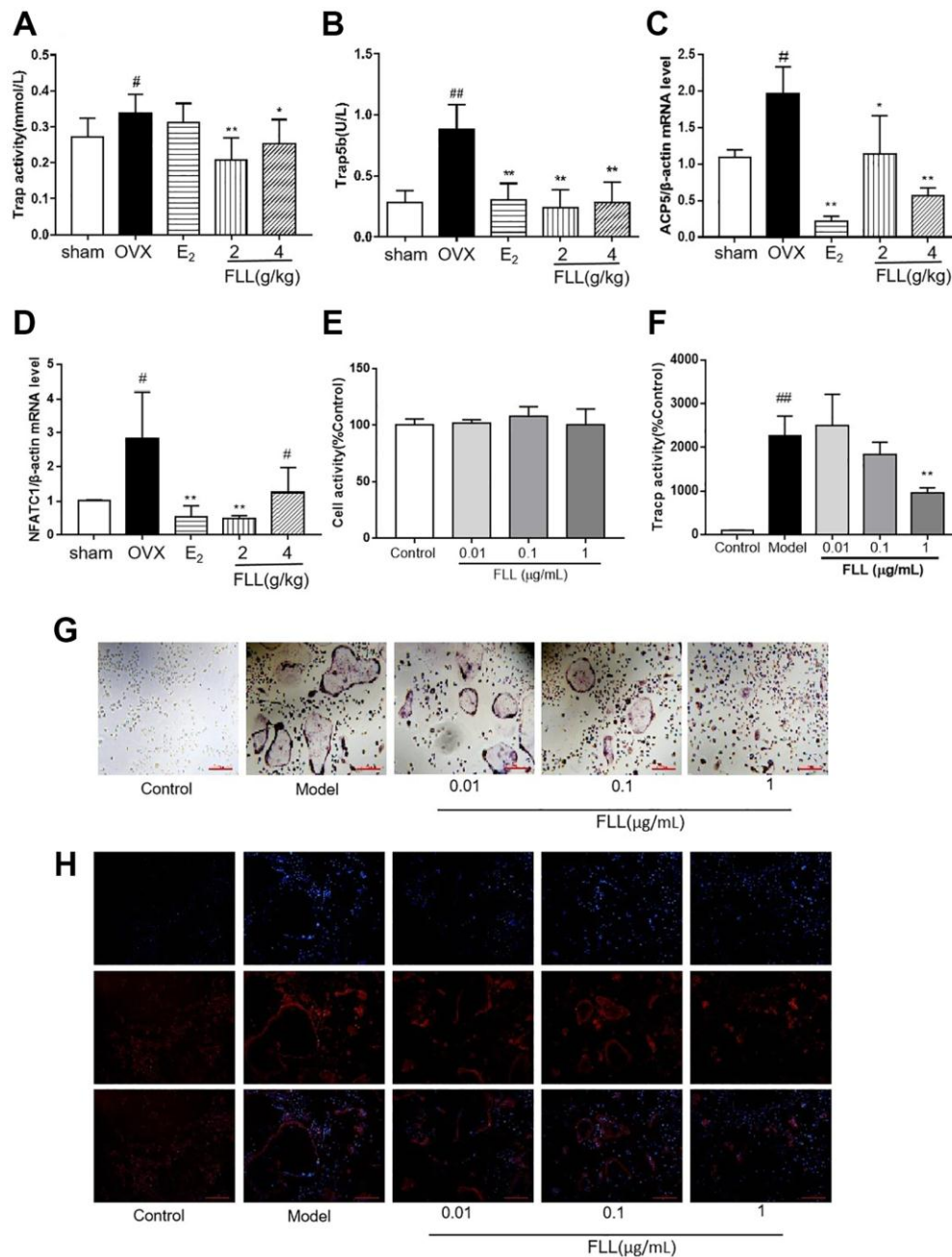


Figure 6. FLL inhibits osteoclastogenesis and function by downregulation of Trap activity and levels of Trap5b and NFATc1. (A–B) The levels of Trap activity and Trap-5b proteins in plasma markedly decreased after treatment with FLL ($n = 10$). (C–D) Trap mRNA expression in the OVX group was significantly higher than in the sham group. Estrogen and FLL suppressed the increase in ACP5 and NFATc1 mRNA expression. ($n = 3$). (E) Monocytes from bone marrow were cultured with M-CSF (2.5 μ g/mL) and FLL seven days before being subjected to CCK-8 assay. (F) The monocytes were treated with M-CSF (2.5 μ g/mL) and RANKL (5 μ g/mL) for 7 days and assessed by tartrate-resistant acid phosphatase (Tracp). FLL (1 μ g/mL) significantly suppressed Tracp activity. ($n = 6$). (G–H) Monocytes were treated with M-CSF (2.5 μ g/mL) and RANKL (5 μ g/mL) for 7 days and stained for Tracp and F-actin rings. [#] $P < 0.05$ compared with sham; ^{##} $P < 0.01$ compared with sham; ^{*} $P < 0.05$ compared with OVX; ^{**} $P < 0.01$ compared with OVX ($n = 3$).

the purpose of black hair. Studies have shown that FLL can be used in the prevention and treatment of menopausal osteoporosis, and increases the content of estrogen in the body and provides estrogenic effects [15]. In the present study, we used the OVX mouse

model to examine the effects of FLL on various organs, and found that FLL reversed OVX-induced uterine atrophy (Figure 1B). This suggested to us that FLL might possess a potential estrogen-like effect, although this requires further investigation.

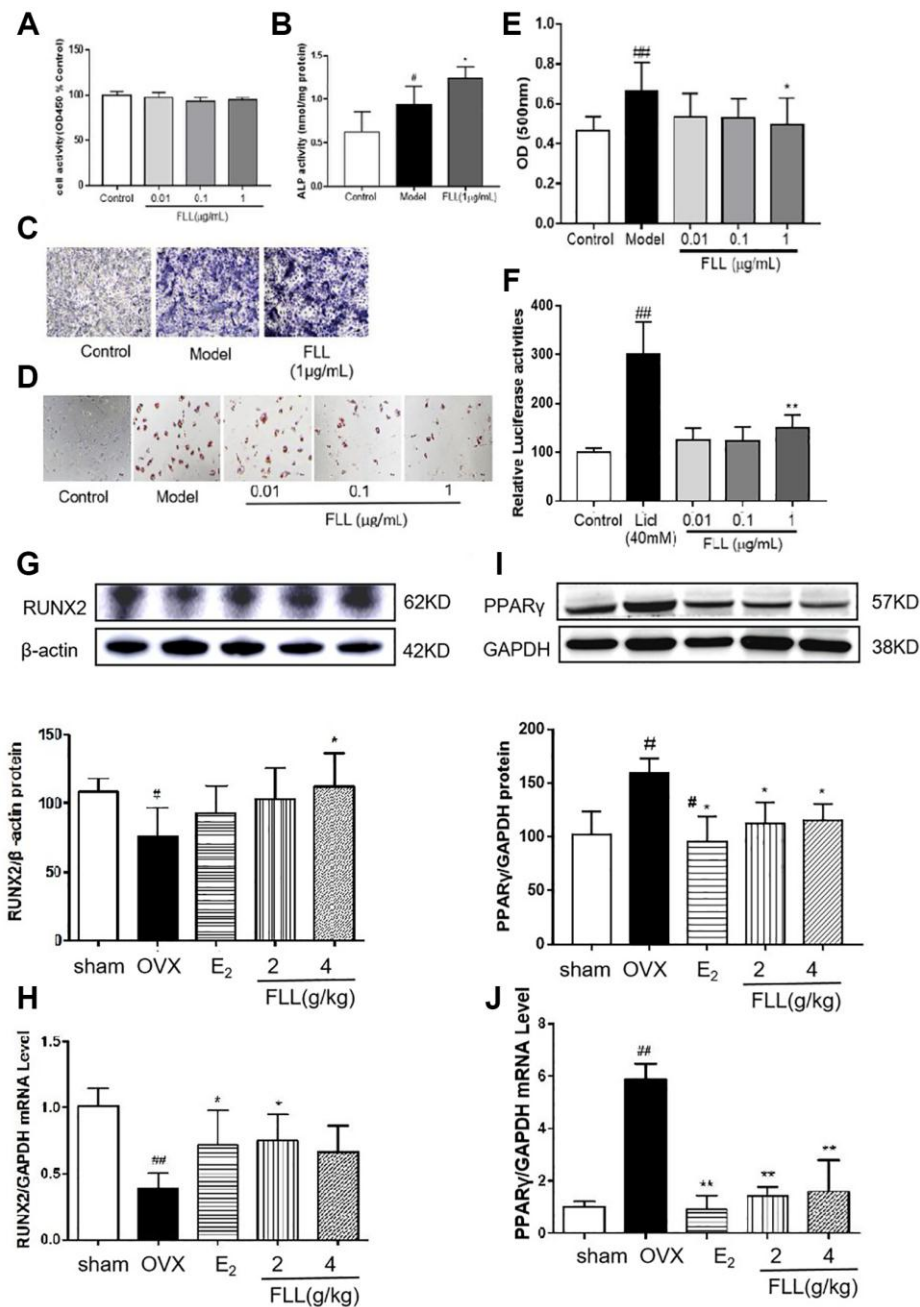


Figure 7. FLL significantly stimulates osteoblast differentiation and inhibits adipocyte differentiation of MSC. (A) The MSC were cultured with FLL and subjected to CCK-8 assay ($n = 6$). (B–C) MSC were cultured with osteogenic-inducer solution for 7 days and we then determined ALP activity, and ALP was also stained with BCIP/NBT; FLL markedly promoted the expression of ALP. ($n = 6$). (D) The MSC were cultured with adipocyte-inducer solution for 7 days and stained with Oil Red. (E) We quantified Oil Red by dissolving it in isopropanol and measuring the absorbance at 500 nm. FLL significantly inhibited adipocyte differentiation ($n = 6$). (F) TOPFlash assay was used to investigate the activation of the Wnt-signaling pathway by FLL, and results showed that FLL significantly activated Wnt signaling ($n = 6$). (G–H) The levels of RUNX2 protein and mRNA in mouse bone marrow were noticeably increased after treatment with FLL ($n = 3$). (I–J) The levels of PPAR γ protein and mRNA in mouse bone marrow were notably decreased after treatment with FLL. ($n = 3$). # $P < 0.05$ compared with sham or control; ## $P < 0.01$ compared with sham or control; * $P < 0.05$ compared OVX or model; ** $P < 0.01$ compared OVX or Licl.

Many investigators have determined that significant physiologic changes are to be found in menopausal women, including an increase in visceral adiposity and a decrease in bone mass. These changes are major risk factors for osteoporosis, obesity, diabetes, and cardiovascular diseases [16–17]; and a large number of studies revealed that estrogen deficiency was related to bone loss and fat accumulation [18]. The Women’s Health Initiative (WHI) publicized in 2002 showed that estrogen treatment increased BMD at multiple sites, and that estrogen treatment also reduced the risk of fractures by 24%. A systematic review showed that estrogen-only therapy, compared with placebo, posed a significantly low risk of fractures [19]. It was reported in a Nature publication that blocking FSH induced thermogenic adipose tissue and reduced body fat, and that a decline in circulating estrogen levels caused a marked increase in circulating FSH levels; this could then explain the obesity prevalent in menopausal women [20]. Therefore, osteoporosis and overweight due to increased fatty tissues are two important and commonly occurring

metabolic? alterations that occur in postmenopausal women. In the present study, we found that FLL significantly reversed OVX-induced bone loss and the increase in fat, while FLL had no effect on lean body mass, liver, spleen, or kidney after administration of FLL for 8 weeks (Figure 2). Since the body weight gained upon OVX was significantly inhibited (Figure 2A), we measured the daily diets for each group (Table 2), and our results showed that the inhibition of body weight with FLL was not dependent upon daily dietary considerations. Therefore, our study potentially provides a novel medical treatment for menopause-related metabolic diseases such as PMOP and postmenopausal weight gain.

Bone remodeling is a complex process that involves bone resorption and bone formation in the body [21]. A balance between bone resorption by osteoclasts and bone formation by osteoblasts is thus essential for maintaining proper bone metabolism and bone mineral density. Conventional scientific wisdom states that

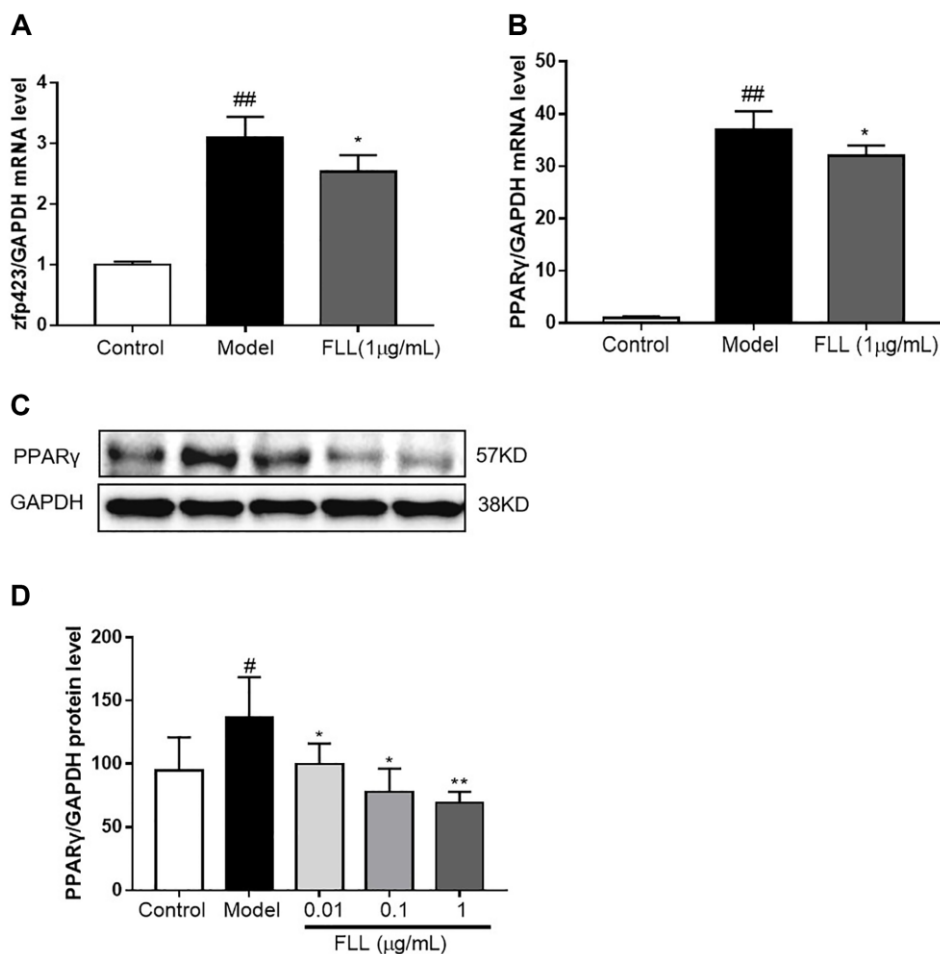


Figure 8. FLL inhibits the maturation of adipocytes but not of preadipocytes. (A) The MSC were cultured with adipocyte-inducer solution for 1 day, and FLL did not increase zfp423 mRNA expression. (B–D) Incubation with FLL for 7 days significantly inhibited the level of PPAR γ mRNA and protein. [#]*P* < 0.05 compared with control; ^{##}*P* < 0.01 compared with control; ^{*}*P* < 0.05 compared with the model; ^{**}*P* < 0.01 compared with the model (*n* = 3).

osteoclasts are the bone-resorption cells found naturally in the body, and they are characterized as large multinucleated cells that are derived from the monocyte/macrophage lineage. The increased number and activity of osteoclasts are responsible for bone destruction in abnormal metabolic bone diseases, such as osteoporosis, osteoarthritis, and malignant tumors [22–24]. Therefore, inhibiting osteoclastogenesis will likely yield a noteworthy therapeutic contribution to the treatment of osteoporosis. We herein demonstrated that FLL reversed the induction of osteoclast activity by RANKL-induced osteoclast differentiation *in vitro*. After 8 weeks of treatment with FLL, the levels of Trap and Trap5b (which are widely regarded as markers of osteoclast activity clinically) [25] decreased significantly in the plasma as determined by ELISA, demonstrating that osteoclast activity was inhibited. In addition, numerous studies have shown that the RANK/RANKL/OPG-signaling pathway plays a crucial role in bone remodeling [26]. RANKL promotes osteoclast precursor-cell differentiation into mature osteoclasts by binding to RANK in the cytoplasmic membrane [27]; and OPG secreted by osteoblasts competitively binds to RANKL and blocks the activation of RANK/RANKL, thus inhibiting the maturation and differentiation of osteoclasts [28]. We also ascertained that FLL increased the expression of OPG and decreased the expression of RANKL in plasma (Figure 3). Hence, the anti-osteoporotic effect of FLL might be achieved by inhibiting osteoclast differentiation through the RANK/RANKL/OPG-signaling pathway. In addition, our research showed that treatment with FLL extract (1 µg/mL) significantly inhibited osteoclast differentiation from bone marrow monocytes in mice, as well as the formation of F-actin rings (Figure 4). The F-actin ring is anchored to the mineralized matrix to form a closed bone-resorption chamber, which is a requisite structure in the maturation of functional osteoclasts [29–30]. Therefore, our study displayed a significant inhibition of osteoclast activity with FLL both *in vitro* and *in vivo*.

Bone formation maintained by osteoblasts is another important aspect of bone remodeling. Bone marrow-derived MSCs constitute a population of multipotent cells in bone marrow [31], and under certain conditions MSCs differentiate into various cells such as osteoblasts, adipose cells, and chondrocytes [32]. Osteogenic and adipogenic differentiation of MSCs are characterized by the two classical markers RUNX2 and PPAR γ , respectively [33], representing a characteristically reciprocal relationship in the bone marrow. When the differentiation of adipose cells increases, the differentiation of osteoblasts decreases accordingly; this reduces the capability for bone formation, destroying the balance between osteoblasts and osteoclasts, leading

to a reduction in bone minerals and bone mass [34–35]. Therefore, it is critically important to maintain bone health by effectively inhibiting differentiation of MSCs toward adipocytes. We suggest that FLL inhibits adipose cell differentiation from MSCs and reduces abdominal fat in OVX mice by decreasing the PPAR γ /RUNX2 ratio (Figure 5). In that respect, the protective effect of FLL on bone metabolism is further improved.

As two common diseases that occur in postmenopausal women, osteoporosis and obesity are both of major public health concern, and the relationship between PMOP and obesity has become an area of intense interest. There are many controversies in publicized studies regarding the effect of fat mass on bone tissues and related fractures. For a long-standing period, researchers believed that obesity was protective against osteoporosis and associated with a decreased risk for fragility fractures because of the protective cushion of fat mass when falling [36]. However, increasing recent evidence revealed that the beneficial effects of fat mass on the entire body or on bone were not identical for all postmenopausal women, and depended upon overall fat distribution [37–38]. There is an increased risk for postmenopausal women to develop visceral obesity [39], and visceral adipose tissue (VAT) is negatively correlated with bone mass. Even after adjustments for age and sex, there remains a statistically significant inverse relationship between VAT and bone [40]. In addition, high VAT and low estrogen negatively affect bone in obese men [41]. Thus, there might be a very close relationship between fat mass and bone. A previous study even showed that fat from bone marrow might be responsible for osteoporosis [42]. In our study, we also found that FLL significantly reversed the increase in bone marrow fat induced by OVX, and this might constitute another mechanism underlying the anti-osteoporotic actions of FLL in the postmenopausal period.

There are two stages of adipogenic differentiation of MSCs. The first stage is the differentiation of preadipocytes, which are morphologically indistinguishable from MSCs but have lost their potential to differentiate into other mesenchymal lineages. The second stage is the terminal differentiation stage, in which the preadipocytes exhibit the characteristics of mature adipocytes; i.e., the capabilities of lipid transport and synthesis, insulin sensitivity, and the secretion of adipokines [43]. *zfp423* is a marker of preadipocytes and perilipin peroxisome proliferator-activated receptor gamma (PPAR γ) is a marker of mature adipocytes [44]. In our study we uncovered increased expression of *Zfp423* and PPAR γ genes in BMSCs after induction by adipogenic supplements for 1 or 7 days. In addition, FLL

significantly inhibited the expression of Zfp423 and PPAR γ mRNAs (Figure 8), suggesting that FLL affects lineage fate determination and terminal differentiation by suppressing adipogenic differentiation of BMSCs.

CONCLUSIONS

Herein we demonstrated that FLL prevented the bone loss induced by estrogen deficiency after 8 weeks using adult female OVX mice. We found an increase in BMD, improvement in bone microstructure, suppression of osteoclast activity, and reduction in fat content in the abdomen and bone marrow. Our findings also indicated that FLL constrained the activity and function of osteoclasts derived from bone marrow mononuclear macrophage cells, stimulated osteoblast differentiation, and inhibited fate determination and maturation of adipocytes. Long-term use of FLL also did not produce any visible side effects. Our current and previous findings strongly indicate that FLL may be clinically useful in the treatment of menopause-related osteoporosis and weight gain.

MATERIALS AND METHODS

Preparation of *Fructus Ligustri Lucidi* (FLL) extracts

FLL was purchased from the medicinal materials market in Anguo, Hebei, and authenticated by Tianjin University of Traditional Chinese Medicine. For the preparation of FLL extracts, 500 g of raw FLL was extracted with 5000 mL of 80% ethanol in a reflux apparatus twice for 2 h each time. After refluxing, the extracts were evaporated in a rotary evaporator and lyophilized in a freeze-dryer. The ultimate extracted yield of FLL was 27.3%.

Animals

Experiments were performed using female C57BL/6 mice (weighing 20–22 g, and at 8 weeks of age) that were purchased from Beijing Weitong Lihua Experimental Animal Technology Co., Ltd., with certificate number SCXX (Beijing) 2016–0006. The mice were maintained under standard specific-pathogen-free (SPF) conditions at the Institute of Radiation Medicine, Chinese Academy of Medical Sciences, at a temperature of 22–25°C, relative humidity of 58–65%, and exposed to a 12-h light/dark cycle; and mice were provided standard food pellets and water ad libitum. Animal care and experimental procedures were approved by the Animal Ethics Committee of the Tianjin University of Traditional Chinese Medicine. All the experiments were performed in accordance with the principles of the NIH (USA) guidelines (NIH publication #85–23, revised in 1985).

After one week of acclimatization, 50 female mice underwent either bilateral laparotomy (sham, $n = 10$) or bilateral ovariectomy (OVX, $n = 40$). The success of OVX was confirmed after 1 week by a significant diminution in plasma estradiol levels. After 1 week of surgery, the mice were randomly assigned to four groups: an OVX group (0.2% Carboxymethylcellulose sodium (CMCNa), $n = 10$), E2 group (estrogen, conjugated estrogens tablets (Xinjiang Xinziyuan Bio-Pharmaceutical Co., Ltd.; H20090172), at 0.039 mg/kg, $n = 10$), FLL group (FLL at 2 g/kg, $n = 10$), and FLL group (FLL at 4 g/kg, $n = 10$). All the animals underwent ovariectomy, except for those in the sham group, which only underwent partial removal of the fat. All the animals were given drugs for 8 weeks by intragastric administration.

Body weight and food intake

We recorded body weights and food intake of all animals every 3–4 days for 8 consecutive weeks after the operation.

Analysis of body composition

The body composition—including body fat content and lean mass—were determined by NMR body-composition analyzer (QMR06-090H, Suzhou Niumai Analytical Instrument Co., Ltd.). The animals underwent isoflurane anesthesia one day before sacrifice.

Indices of uterine morphology in OVX mice

Eight weeks after treatment with FLL, the mice were killed and uteri removed for weighing and photographic examination.

Enzyme-linked immunosorbent (ELISA) assay

The plasma markers of bone turnover—including tartrate-resistant acid phosphatase (Trap), tartrate-resistant acid phosphatase 5b (Trap5b), osteoprotegerin (OPG), and receptor activator of nuclear factor kappa-B ligand (RANKL)—were measured with ELISA kits purchased from CUSABIO (China). Estradiol concentrations in plasma were determined using a kit purchased from R&D Systems (USA), according to the manufacturer's instructions.

Bone mineral density and microstructure

The bone mineral density (BMD) in the left femur was determined by dual-energy X-ray absorptiometry with an InAlyzer instrument (Faxitron Bioptics, USA), and the bone microstructure was analyzed by a microcomputed tomography (micro-CT) system

(SCANCO MicroCT, Switzerland). The left femur was collected and cleaned by removing the attached muscles after sacrifice, and the sample was stored in 10% neutralized formalin.

Left tibial strength

Left tibial strength was measured with a small-animal bone-strength tester (YLS-16A, China). The tibia was placed in the machine and the button was pressed until the tibia fractured, providing the data for tibial strength.

Culture of mesenchymal stem cells from bone marrow

Bone marrow from bilateral femurs and tibiae was flushed with phosphate-buffered saline (PBS) containing a 10% penicillin-streptomycin solution. After filtering through a 70- μ m filter membrane, the filtrate was centrifuged at 300 g for 5 min, and cells were collected and cultured with α -MEM (Gibco; Thermo Fisher Scientific) containing 10% fetal bovine serum (FBS; BI) and 1% penicillin-streptomycin solution (penicillin 100 U/mL and streptomycin 100 μ g/mL; BI). Cells were incubated under 5% CO₂ at 37°C. The culture medium was first changed after 48 h, followed by subsequent replacements with fresh medium every two days. Bone marrow mesenchymal stem cells (BMMSCs) at the third passage were used for experiments.

Adipogenic differentiation *in vitro*

The third-passage BMMSCs were seeded in each well of 96-well plates at a concentration of 10⁵ cells/mL. Adipogenic differentiation medium (comprising dexamethasone, 0.1 μ M; IBMX, 0.5 mM; insulin, 10 μ g/mL; and indomethacin, 200 μ M) was added for 14 days, and cells were then finally stained with Oil Red O (Solarbio; G1260). The control-group cells were treated only with medium (α -MEM supplemented with 10% FBS [BI], penicillin [100 U/mL], and streptomycin [100 μ g/mL, BI]) without the induction solution or the addition of drugs. The experiment was repeated a minimum of three times.

Osteoblast differentiation *in vivo*

The third-passage BMMSCs were seeded in each well of 96-well plates at a concentration of 5 \times 10⁴ cells/mL. Osteoblast differentiation medium (dexamethasone, 0.1 μ M; β -sodium glycerophosphate, 10 mM; and vitamin C, 50 μ M) was added for 7 days, and we stained for alkaline phosphatase (ALP) with BCIP/NBT as chromogenic substrates (Beyotime, C3206). The experiment was repeated a minimum of three times.

Osteoclast culture

The cells were derived from 4-week-old C57BL/6 female mice. Bone marrow from bilateral femurs and tibiae was flushed with PBS containing a 10% penicillin-streptomycin solution, mononuclear cells were isolated with a sterile Ficoll solution, and red blood cells were removed using a red blood cell lysis buffer. The cells were maintained in α -MEM supplemented with 10% FBS (BI), penicillin (100 U/mL), and streptomycin (100 μ g/mL, BI). Incubations were performed at 37°C in 5% CO₂. The cells were seeded in a 96-well plate at 3 \times 10⁵ cells/mL, and after one day macrophage colony-stimulating factor (M-CSF, 2.5 μ g/mL) and receptor activator of NF- κ B ligand (RANKL, 5 μ g/mL) were used to induce osteoclast differentiation. The medium was replaced every three days. The FLL was dissolved in 0.1% dimethyl sulfoxide and further diluted with α -MEM culture medium to an appropriate concentration (0.01, 0.1, and 1 μ g/mL). The experiment was repeated a minimum of three times.

Trap-activity assay and Trap staining

Trap activity was used as a marker of osteoclast differentiation. The cells were seeded on a 96-well plate and induced into osteoclasts. After five days of culture, the medium in the plate was transferred to a new plate for the Trap-activity assay using an Acid Phosphatase Assay Kit (Trap, Beyotime). The cells were washed twice with PBS and fixed with 4% paraformaldehyde for 30 min; we then followed the Trap-staining kit manufacturer's protocol (Sigma-Aldrich). Trap-positive multinuclear cells were identified as those containing more than three nuclei that appeared dark red. The experiment was repeated a minimum of three times.

F-actin staining

After fixing cells with 4% paraformaldehyde for 30 min, we used 0.1% Triton X-100 to permeabilize the cells for 10 min. Cells were then washed twice with PBS and sealed with 1% bovine serum albumin (BSA) for 30 min. The cells were again washed twice with PBS, Alexa Fluor 568 (1:50) was added at 40 μ l/well, and the cells were then incubated at 37°C for 40 min. Hoechst stain was added for 15 min and the cells were kept in the dark. F-actin ring formations were measured by using an inverted fluorescence microscope (Zeiss, Germany). The experiment was repeated at least three times.

Real-time PCR

Total RNA was extracted with the Trizol reagent (Invitrogen Life Technology, Carlsbad, CA), and 1 μ g

Table 2. Names and sequences of primers used for polymerase chain reaction analysis.

Gene	Sequence
GAPDH	F: 5'GGTCGGAGTCAACGGATTTGG3', R: 5'CTCCTGGAAGATGGTGATGGG3'
PPAR γ	F: 5'GGGTAAGCTCTTGTGAATGG3' R: 5'CTGATGCACTGCCTATGAGC3'
Pref-1	F: 5'CCTGGCTGTGTCAATGGAGT3' R: 5'CAAGTTCCATTGTTGGCGCA3'
Zfp-423	F: 5'CGCGATCGGTGAAAGTTGAA3' R: 5'CGATCACACTCTGGCTCTCC3'
ACP5	F: 5'CGATGCCAGCGACAAGAGGTTTC3' R: 5'CTGTGCAGAGACTTGCCAAGG3'
NFATC1	F: 5'ACCACCAGCCACGAGATCATCC3' R: 5'AACTCGGAAGACCAGCCTCACC3'
Runx2	F: 5'-GCGTCAACACCATCATTCTG-3' R: 5'-CAGACCAGCAGCACTCCATC-3'

of RNA was reversed-transcribed to cDNA. Real-time PCR was conducted using a FastStart Universal SYBR Green Master (ROX) mix (Roche, Germany), and amplification was with an ABI Prism 7300 Sequence Detection System. The amplification conditions were an initial 2 min at 95°C and 40 cycles of denaturation at 95°C for 15 s, annealing at 65°C for 60 s, and extension at 72°C for 15 s. The results were calculated using the $2^{-\Delta\Delta C_t}$ method. Primer sequences are depicted in Table 2.

Western immunoblotting analysis

The protein from bone marrow was extracted using a 1-mL syringe containing PBS, and red blood cell (RBC) lysis buffer (RIPA, Solarbio) was added to lyse the RBCs (PMSF = 100:1; Solarbio, R0020, P0100) on ice for 10 min. Total protein was extracted from cells using the lysis buffer directly. Next, the suspension was centrifuged at 12,000 g for 10 min at 4°C, and the supernatant was collected into a new centrifuge tube for later use. Total protein concentration was determined by using the Pierce Rapid Gold BCA Protein Assay Kit (Thermo Fisher; A53225), following the manufacturer's protocol. The expression of target proteins was detected using SDS-PAGE (40 μ g of total protein per well), with electrophoresis performed at 50 V for 30 min and at 100 V for 1 h; and then proteins were transferred onto PVDF membranes (Millipore). The membranes were blocked with 5% nonfat dried milk in TBST (0.5% Tween in TBS) for 2 h and then incubated overnight at 4°C with rabbit polyclonal antibody diluted 1:1000 with TBST (RUNX2, Abcam, ab76056; OPG, Abcam, ab203061; RANKL, Absin, abs120177; PPAR γ , Affinity, AF6284). The next day, the membranes were washed three times for 5 min each time with TBST and incubated with an appropriate secondary antibody

(ZB2301; 1:10,000) at room temperature for 2 h. The protein bands were visualized using ECL western blotting substrate (P90719, Millipore) and exposed with a ChemiDoc MP Imaging System (BIO-RAD, 734BR4251). Protein expression level was defined with the gel imaging analysis system ImageJ (National Institutes of Health, USA), and normalized with the corresponding β -actin or GAPDH as the internal control.

Statistical analysis

We used IBM SPSS Statistics for Windows (version 22; SPSS Inc., Chicago, IL, USA) for statistical analysis, and constructed graphs using GraphPad Prism (version 7.0 for Windows, GraphPad Software, LaJolla, California USA). The values are all expressed as mean \pm SD. Student's *t*-test was used to compare the means of two groups. When ≥ 3 groups were specifically compared, we used one-way ANOVA. A *p*-value < 0.05 was considered statistically significant.

Abbreviations

ACP5: acid phosphatase 5; ALP: alkaline phosphatase; BMD: bone mineral density; BMSCs: bone marrow mesenchymal stem cells; BSA: bovine serum albumin; CCK-8: Cell Counting Kit-8; Conn.D: connectivity density; E2: estrogen; ELISA: enzyme-linked immunosorbent assay; FBS: fetal bovine serum; FLL: *Fructus Ligustri Lucidi*; M-CSF: macrophage colony-stimulating factor; NFATC1: nuclear factor of activated T cells 1; OPG: osteoprotegerin; OVX: ovariectomy; PBS: phosphate-buffered saline; PCR: polymerase chain reaction; PMOP: postmenopausal osteoporosis; PPAR: peroxisome proliferator-activated receptor

gamma; RANKL: receptor activator of NF- κ B ligand; RUNX2: RUNX family transcription factor 2; TCM: traditional Chinese medicine; Trap: tartrate-resistant acid phosphatase; Trap5b: tartrate-resistant acid phosphatase 5b; VAT: visceral adipose tissue; Zfp423: zinc-finger protein 423.

AUTHOR CONTRIBUTIONS

Haoping Mao designed the research; Xiaoyan Qin, Qiu Wei, and Yun Yang wrote the manuscript and performed the experimental work; and Xiaoling Han and Ran An analyzed the data. All authors discussed, edited, and approved the final version.

CONFLICTS OF INTEREST

The authors declare no conflicts of interest related to this study.

FUNDING

This work was supported by grants from the National Natural Science Foundation of China (No. 81630106), the Graduate Research and Innovation Project of Tianjin (No. 2019YJSB140; YJSKC-20191002).

REFERENCES

1. Eastell R, Rosen CJ. Response to Letter to the Editor: "Pharmacological Management of Osteoporosis in Postmenopausal Women: An Endocrine Society Clinical Practice Guideline". *J Clin Endocrinol Metab*. 2019; 104:3537–38. <https://doi.org/10.1210/jc.2019-00777> PMID:30998238
2. Greco EA, Lenzi A, Migliaccio S. The obesity of bone. *Ther Adv Endocrinol Metab*. 2015; 6:273–86. <https://doi.org/10.1177/2042018815611004> PMID:26623005
3. O'Leary DP, Murray FE, Turner BS, LaMont JT. Bile salts stimulate glycoprotein release by guinea pig gallbladder in vitro. *Hepatology*. 1991; 13:957–61. PMID:2030000
4. van Gemert WA, Peeters PH, May AM, Doornbos AJH, Elias SG, van der Palen J, Veldhuis W, Stapper M, Schuit JA, Monnikhof EM. Effect of diet with or without exercise on abdominal fat in postmenopausal women - a randomised trial. *BMC Public Health*. 2019; 19:174. <https://doi.org/10.1186/s12889-019-6510-1> PMID:30744621
5. Gao L, Li C, Wang Z, Liu X, You Y, Wei H, Guo T. *Ligustri lucidi fructus* as a traditional Chinese medicine: a review of its phytochemistry and pharmacology. *Nat Prod Res*. 2015; 29:493–510. <https://doi.org/10.1080/14786419.2014.954114> PMID:25244978
6. Qin XY, Niu ZC, Han XL, Yang Y, Wei Q, Gao XX, An R, Han LF, Yang WZ, Chai LJ, Liu EW, Gao XM, Mao HP. Anti-perimenopausal osteoporosis effects of Erzhi formula via regulation of bone resorption through osteoclast differentiation: A network pharmacology-integrated experimental study. *J Ethnopharmacol*. 2021; 270:113815. <https://doi.org/10.1016/j.jep.2021.113815> PMID:33444724
7. Chow SK, Leung KS, Qin J, Guo A, Sun M, Qin L, Cheung WH. Mechanical stimulation enhanced estrogen receptor expression and callus formation in diaphyseal long bone fracture healing in ovariectomy-induced osteoporotic rats. *Osteoporos Int*. 2016; 27:2989–3000. <https://doi.org/10.1007/s00198-016-3619-2> PMID:27155884
8. Fan JZ, Yang L, Meng GL, Lin YS, Wei BY, Fan J, Hu HM, Liu YW, Chen S, Zhang JK, He QZ, Luo ZJ, Liu J. Estrogen improves the proliferation and differentiation of hBMSCs derived from postmenopausal osteoporosis through notch signaling pathway. *Mol Cell Biochem*. 2014; 392:85–93. <https://doi.org/10.1007/s11010-014-2021-7> PMID:24752351
9. Shang H, Zhou A, Jiang J, Liu Y, Xie J, Li S, Chen Y, Zhu X, Tan H, Li J. Inhibition of the fibrillation of highly amyloidogenic human calcitonin by cucurbit[7]uril with improved bioactivity. *Acta Biomater*. 2018; 78:178–88. <https://doi.org/10.1016/j.actbio.2018.07.045> PMID:30076991
10. Xiao YP, Zeng J, Jiao LN, Xu XY. [Review for treatment effect and signaling pathway regulation of kidney-tonifying traditional Chinese medicine on osteoporosis]. *Zhongguo Zhong Yao Za Zhi*. 2018; 43:21–30. <https://doi.org/10.19540/j.cnki.cjcmm.20171106.002> PMID:29552807
11. Giuliani N, Colla S, Morandi F, Barille-Nion S, Rizzoli V. Lack of receptor activator of nuclear factor- κ B ligand (RANKL) expression and functional production by human multiple myeloma cells. *Haematologica*. 2005; 90:275–78. PMID:15710592
12. Wu R, Li Q, Pei X, Hu K. Effects of Brucine on the OPG/RANKL/RANK Signaling Pathway in MDA-MB-231 and MC3T3-E1 Cell Coculture System. *Evid Based Complement Alternat Med*. 2017; 2017:1693643.

- <https://doi.org/10.1155/2017/1693643>
PMID:[29081815](https://pubmed.ncbi.nlm.nih.gov/29081815/)
13. Wang F, Liu Z, Lin S, Lu H, Xu J. Icariin enhances the healing of rapid palatal expansion induced root resorption in rats. *Phytomedicine*. 2012; 19:1035–41. <https://doi.org/10.1016/j.phymed.2012.06.001>
PMID:[22818561](https://pubmed.ncbi.nlm.nih.gov/22818561/)
 14. Brömme D, Lecaille F. Cathepsin K inhibitors for osteoporosis and potential off-target effects. *Expert Opin Investig Drugs*. 2009; 18:585–600. <https://doi.org/10.1517/13543780902832661>
PMID:[19388876](https://pubmed.ncbi.nlm.nih.gov/19388876/)
 15. Bonnet N, Brun J, Rousseau JC, Duong LT, Ferrari SL. Cathepsin K Controls Cortical Bone Formation by Degrading Periostin. *J Bone Miner Res*. 2017; 32:1432–41. <https://doi.org/10.1002/jbmr.3136>
PMID:[28322464](https://pubmed.ncbi.nlm.nih.gov/28322464/)
 16. Saleh N, Nassef NA, Shawky MK, Elshishiny MI, Saleh HA. Novel approach for pathogenesis of osteoporosis in ovariectomized rats as a model of postmenopausal osteoporosis. *Exp Gerontol*. 2020; 137:110935. <https://doi.org/10.1016/j.exger.2020.110935>
PMID:[32339647](https://pubmed.ncbi.nlm.nih.gov/32339647/)
 17. Kase NG, Gretz Friedman E, Brodman M. The midlife transition and the risk of cardiovascular disease and cancer Part II: strategies to maximize quality of life and limit dysfunction and disease. *Am J Obstet Gynecol*. 2020; 223:834–47.e2. <https://doi.org/10.1016/j.ajog.2020.06.008>
PMID:[32533929](https://pubmed.ncbi.nlm.nih.gov/32533929/)
 18. Jang SA, Hwang YH, Kim T, Yang H, Lee J, Seo YH, Park JI, Ha H. Water Extract of *Agastache rugosa* Prevents Ovariectomy-Induced Bone Loss by Inhibiting Osteoclastogenesis. *Foods*. 2020; 9:1181. <https://doi.org/10.3390/foods9091181>
PMID:[32858922](https://pubmed.ncbi.nlm.nih.gov/32858922/)
 19. Gartlehner G, Patel SV, Feltner C, Weber RP, Long R, Mullican K, Boland E, Lux L, Viswanathan M. Hormone Therapy for the Primary Prevention of Chronic Conditions in Postmenopausal Women: Evidence Report and Systematic Review for the US Preventive Services Task Force. *JAMA*. 2017; 318:2234–49. <https://doi.org/10.1001/jama.2017.16952>
PMID:[29234813](https://pubmed.ncbi.nlm.nih.gov/29234813/)
 20. Liu P, Ji Y, Yuen T, Rendina-Ruedy E, DeMambro VE, Dhawan S, Abu-Amer W, Izadmehr S, Zhou B, Shin AC, Latif R, Thangeswaran P, Gupta A, et al. Blocking FSH induces thermogenic adipose tissue and reduces body fat. *Nature*. 2017; 546:107–12. <https://doi.org/10.1038/nature22342>
PMID:[28538730](https://pubmed.ncbi.nlm.nih.gov/28538730/)
 21. Peyroteo MMA, Belinha J, Natal Jorge RM. A mathematical biomechanical model for bone remodeling integrated with a radial point interpolating meshless method. *Comput Biol Med*. 2021; 129:104170. <https://doi.org/10.1016/j.combiomed.2020.104170>
PMID:[33352308](https://pubmed.ncbi.nlm.nih.gov/33352308/)
 22. Yu P, Xu Z, Zhai X, Liu Y, Sun H, Xu X, Xie J, Li J. Supramolecular nanoassemblies of salmon calcitonin and aspartame for fibrillation inhibition and osteogenesis improvement. *Int J Pharm*. 2021; 593:120171. <https://doi.org/10.1016/j.ijpharm.2020.120171>
PMID:[33321170](https://pubmed.ncbi.nlm.nih.gov/33321170/)
 23. Duan L, Liang Y, Xu X, Wang J, Li X, Sun D, Deng Z, Li W, Wang D. Noncoding RNAs in subchondral bone osteoclast function and their therapeutic potential for osteoarthritis. *Arthritis Res Ther*. 2020; 22:279. <https://doi.org/10.1186/s13075-020-02374-x>
PMID:[33239099](https://pubmed.ncbi.nlm.nih.gov/33239099/)
 24. Stopeck AT. Osteoclast inhibition in postmenopausal breast cancer: Is the evidence too strong to ignore? *Cancer*. 2017; 123:2392–94. <https://doi.org/10.1002/cncr.30678>
PMID:[28464216](https://pubmed.ncbi.nlm.nih.gov/28464216/)
 25. Rajfer RA, Flores M, Abraham A, Garcia E, Hinojosa N, Desai M, Artaza JN, Ferrini MG. Prevention of Osteoporosis in the Ovariectomized Rat by Oral Administration of a Nutraceutical Combination That Stimulates Nitric Oxide Production. *J Osteoporos*. 2019; 2019:1592328. <https://doi.org/10.1155/2019/1592328>
PMID:[31275540](https://pubmed.ncbi.nlm.nih.gov/31275540/)
 26. de Castro LF, Burke AB, Wang HD, Tsai J, Florenzano P, Pan KS, Bhattacharyya N, Boyce AM, Gafni RI, Molinolo AA, Robey PG, Collins MT. Activation of RANK/RANKL/OPG Pathway Is Involved in the Pathophysiology of Fibrous Dysplasia and Associated With Disease Burden. *J Bone Miner Res*. 2019; 34:290–94. <https://doi.org/10.1002/jbmr.3602>
PMID:[30496606](https://pubmed.ncbi.nlm.nih.gov/30496606/)
 27. Ikebuchi Y, Aoki S, Honma M, Hayashi M, Sugamori Y, Khan M, Kariya Y, Kato G, Tabata Y, Penninger JM, Udagawa N, Aoki K, Suzuki H. Coupling of bone resorption and formation by RANKL reverse signalling. *Nature*. 2018; 561:195–200. <https://doi.org/10.1038/s41586-018-0482-7>
PMID:[30185903](https://pubmed.ncbi.nlm.nih.gov/30185903/)
 28. Liu C, Chen X, Zhi X, Weng W, Li Q, Li X, Zou Y, Su J, Hu HG. Structure-based development of an osteoprotegerin-like glycopeptide that blocks RANKL/RANK interactions and reduces ovariectomy-

- induced bone loss in mice. *Eur J Med Chem.* 2018; 145:661–72.
<https://doi.org/10.1016/j.ejmech.2018.01.022>
PMID:[29348072](https://pubmed.ncbi.nlm.nih.gov/29348072/)
29. Liu Z, Li Y, Guo F, Zhang C, Song G, Yang J, Chen D. Tetrandrine Inhibits Titanium Particle-Induced Inflammatory Osteolysis through the Nuclear Factor- κ B Pathway. *Mediators Inflamm.* 2020; 2020:1926947.
<https://doi.org/10.1155/2020/1926947>
PMID:[33312069](https://pubmed.ncbi.nlm.nih.gov/33312069/)
30. Li L, Sapkota M, Gao M, Choi H, Soh Y. Macrolactin F inhibits RANKL-mediated osteoclastogenesis by suppressing Akt, MAPK and NFATc1 pathways and promotes osteoblastogenesis through a BMP-2/smad/Akt/Runx2 signaling pathway. *Eur J Pharmacol.* 2017; 815:202–09.
<https://doi.org/10.1016/j.ejphar.2017.09.015>
PMID:[28919027](https://pubmed.ncbi.nlm.nih.gov/28919027/)
31. Georgiou KR, Scherer MA, Fan CM, Cool JC, King TJ, Foster BK, Xian CJ. Methotrexate chemotherapy reduces osteogenesis but increases adipogenic potential in the bone marrow. *J Cell Physiol.* 2012; 227:909–18.
<https://doi.org/10.1002/jcp.22807>
PMID:[21503894](https://pubmed.ncbi.nlm.nih.gov/21503894/)
32. Ji K, Ding L, Chen X, Dai Y, Sun F, Wu G, Lu W. Mesenchymal Stem Cells Differentiation: Mitochondria Matter in Osteogenesis or Adipogenesis Direction. *Curr Stem Cell Res Ther.* 2020; 15:602–06.
<https://doi.org/10.2174/1574888X15666200324165655>
PMID:[32208124](https://pubmed.ncbi.nlm.nih.gov/32208124/)
33. Jang HJ, Lim S, Kim JM, Yoon S, Lee CY, Hwang HJ, Shin JW, Shin KJ, Kim HY, Park KI, Nam D, Lee JY, Yea K, et al. Glucosylceramide synthase regulates adipogenic differentiation through synergistic activation of PPAR γ with GlcCer. *FASEB J.* 2020; 34:1270–87.
<https://doi.org/10.1096/fj.201901437R>
PMID:[31914593](https://pubmed.ncbi.nlm.nih.gov/31914593/)
34. Yu B, Huo L, Liu Y, Deng P, Szymanski J, Li J, Luo X, Hong C, Lin J, Wang CY. PGC-1 α Controls Skeletal Stem Cell Fate and Bone-Fat Balance in Osteoporosis and Skeletal Aging by Inducing TAZ. *Cell Stem Cell.* 2018; 23:615–23.
<https://doi.org/10.1016/j.stem.2018.09.001>
PMID:[30244868](https://pubmed.ncbi.nlm.nih.gov/30244868/)
35. Griffith JF, Yeung DK, Antonio GE, Wong SY, Kwok TC, Woo J, Leung PC. Vertebral marrow fat content and diffusion and perfusion indexes in women with varying bone density: MR evaluation. *Radiology.* 2006; 241:831–38.
<https://doi.org/10.1148/radiol.2413051858>
PMID:[17053202](https://pubmed.ncbi.nlm.nih.gov/17053202/)
36. Albala C, Yáñez M, Devoto E, Sostin C, Zeballos L, Santos JL. Obesity as a protective factor for postmenopausal osteoporosis. *Int J Obes Relat Metab Disord.* 1996; 20:1027–32.
PMID:[8923160](https://pubmed.ncbi.nlm.nih.gov/8923160/)
37. Crivelli M, Chain A, da Silva ITF, Waked AM, Bezerra FF. Association of Visceral and Subcutaneous Fat Mass With Bone Density and Vertebral Fractures in Women With Severe Obesity. *J Clin Densitom.* 2021; 24:397–405.
<https://doi.org/10.1016/j.jocd.2020.10.005>
PMID:[33109469](https://pubmed.ncbi.nlm.nih.gov/33109469/)
38. Loh WJ, Stevenson JC, Godsland IF. Independent relationships between bone mineral density, regional body fat and insulin sensitivity in white males. *Clin Endocrinol (Oxf).* 2019; 91:63–71.
<https://doi.org/10.1111/cen.13989>
PMID:[30973644](https://pubmed.ncbi.nlm.nih.gov/30973644/)
39. Anagnostis P, Paschou SA, Katsiki N, Krikidis D, Lambrinou I, Goulis DG. Menopausal Hormone Therapy and Cardiovascular Risk: Where are we Now? *Curr Vasc Pharmacol.* 2019; 17:564–72.
<https://doi.org/10.2174/1570161116666180709095348>
PMID:[29984659](https://pubmed.ncbi.nlm.nih.gov/29984659/)
40. Zhang P, Peterson M, Su GL, Wang SC. Visceral adiposity is negatively associated with bone density and muscle attenuation. *Am J Clin Nutr.* 2015; 101:337–43.
<https://doi.org/10.3945/ajcn.113.081778>
PMID:[25646331](https://pubmed.ncbi.nlm.nih.gov/25646331/)
41. Orstrup MJ, Kjær TN, Harsløf T, Stødkilde-Jørgensen H, Hougaard DM, Cohen A, Pedersen SB, Langdahl BL. Adipose tissue, estradiol levels, and bone health in obese men with metabolic syndrome. *Eur J Endocrinol.* 2015; 172:205–16.
<https://doi.org/10.1530/EJE-14-0792>
PMID:[25416724](https://pubmed.ncbi.nlm.nih.gov/25416724/)
42. Wong AK, Chandrakumar A, Whyte R, Reitsma S, Gillick H, Pokhoy A, Papaioannou A, Adachi JD. Bone Marrow and Muscle Fat Infiltration Are Correlated among Postmenopausal Women With Osteoporosis: The AMBERS Cohort Study. *J Bone Miner Res.* 2020; 35:516–27.
<https://doi.org/10.1002/jbmr.3910>
PMID:[31675452](https://pubmed.ncbi.nlm.nih.gov/31675452/)
43. Liu H, Li J, Lu D, Li J, Liu M, He Y, Williams BO, Li J, Yang T. Ginkgolic acid, a sumoylation inhibitor, promotes adipocyte commitment but suppresses adipocyte terminal differentiation of mouse bone marrow stromal cells. *Sci Rep.* 2018; 8:2545.
<https://doi.org/10.1038/s41598-018-20244-0>
PMID:[29416046](https://pubmed.ncbi.nlm.nih.gov/29416046/)

44. Liu SY, Zhang YY, Gao Y, Zhang LJ, Chen HY, Zhou Q, Chai ML, Li QY, Jiang H, Yuan B, Dai LS, Zhang JB. MiR-378 Plays an Important Role in the Differentiation of Bovine Preadipocytes. *Cell Physiol Biochem*. 2015; 36:1552–62.
<https://doi.org/10.1159/000430318>
PMID:[26159460](https://pubmed.ncbi.nlm.nih.gov/26159460/)